Science Bulletin 64 (2019) 534–539

Contents lists available at ScienceDirect

Science Bulletin

journal homepage: www.elsevier.com/locate/scib

Article

What is the mass of loess in the Loess Plateau of China?

Yuanjun Zhu [a,c,d,*,1], Xiaoxu Jia [b,d,1], Jiangbo Qiao [a], Ming'an Shao [a,b,c,d]

[a] State Key Laboratory of Soil Erosion and Dryland Farming on the Loess Plateau, Northwest A&F University, Yangling 712100, China
[b] Key Laboratory of Ecosystem Network Observation and Modeling, Institute of Geographic Sciences and Natural Resources Research, Chinese Academy of Sciences, Beijing 100101, China
[c] Institute of Soil and Water Conservation, Chinese Academy of Sciences & Ministry of Water Resources, Yangling 712100, China
[d] College of Resources and Environment, University of Chinese Academy of Sciences, Beijing 100190, China

ARTICLE INFO

Article history:
Received 21 January 2019
Received in revised form 12 March 2019
Accepted 13 March 2019
Available online 22 March 2019

Keywords:
The Loess Plateau
Loess mass
Pedotransfer function
Soil erosion
Bulk density

ABSTRACT

The Loess Plateau of China (LP) has the largest and thickest loess deposits in the world. Quantifying the amount of loess in the LP is crucial for investigating the accumulation and erosion of loess, and determining the regional soil and water resource capacity. We used loess thickness data, a pedotransfer function for bulk density (BD), and the clay content data observed in 242 sites across the LP to derive the BD of loess and then estimate the loess mass and its distribution across the LP. The results indicated that the average BD of loess between the surface and bedrock is 1.58 g cm^{-3}, varying from 1.18 to 1.87 g cm^{-3}. The total loess mass is approximately 5.45×10^{13} t, and the average loess mass over an area of 1 m^2 is 169 t, ranging from 1.36 to 585 t. The greatest mass of loess is in the south-central of the LP while the lowest mass of loess is in the northwest and river valley areas. Our estimate of loess mass provides key data for calculating water, carbon, and nutrient storages in the LP, which improves our understanding of soil-water processes and ecohydrological systems in this landscape.

1. Introduction

Soil including sediments on the bedrock is a pivotal natural resource and a key ecosystem component that supply water and nutrients to plants [1–3]. However, the soil is easily displaced under external forces such as water, wind, and gravity, forming soil erosion [4]. With the effects of climate change and human activities, soil erosion is becoming increasingly prevalent worldwide, especially in areas that are ecologically fragile and rapidly urbanized [5–10]. It is estimated that the natural (geological) soil erosion rate is 0.173 mm a^{-1}, but it can be as high as 3.939 mm a^{-1} in conventional agriculture [11]. As a result, 7.5×10^9 t of soil is removed from the land every year, and nearly one-third of the world's arable land has been lost due to soil erosion in the last 40 years [12]. Because erosion removed surface soil, it results in a thinning of soil and loss of water and nutrients, and consequently damages the ecosystem [8,11,12]. Therefore, the amount of soil in an area (expressed in terms of its mass or volume) is a benchmark for soil erosion and closely related to the health of the ecosystem.

The Loess Plateau of China (LP) has the largest and thickest loess deposits around the world and is currently facing a variety of soil erosion, vegetation and land use changes, which threaten fragile ecosystems and result in shortages in water resources [13–16]. Loess is a clastic, predominantly silt-sized sediment that is formed by the accumulation of wind-blown dust, and 10% of the Earth's land area is covered by loess and similar deposits [17,18]. The Yuan (a protruding flat and large plain), Liang (a convex and long ridge), and Mao (a conical hill) features in the LP are formed mainly by soil erosion. Thus, the relationship between soil erosion and landforms needs to be explored to elucidate the evolution of the LP's topography. The annual average sediment of the Yellow River Basin into the sea is 2.56×10^8 t a^{-1} (1987–2015), most of which comes from the LP [19]. Determining the accumulation and erosion rates of loess is the basis for addressing the change of sediment transport and calculating the threshold of soil loss tolerance in the LP [6,20–22]. The mass of loess is central to solving the above problems and can also provide boundary conditions for soil erosion numerical simulations. All of these contribute to the conservation of soil and water resources and soil erosion control.

Soil stores water, carbon, and nutrients [23–25]. When the "Grain for Green" project was implemented in the LP in 1999, water stored in the loess became essential for sustaining vegetation and calculating the potential of vegetation restoration [5,19]. This water is also the main source of groundwater recharge and evapotranspiration, usually estimated by in-situ observations and isotope techniques [15,26]. However, limited observation sites

* Corresponding author.
E-mail address: zhuyj@nwsuaf.edu.cn (Y. Zhu).
[1] These authors contributed equally to this work.

https://doi.org/10.1016/j.scib.2019.03.021
2095-9273/

and the shortcomings of isotope techniques make it difficult to obtain comprehensive and reliable estimates of water storage. Loess mass combined with soil moisture can be used to easily and accurately estimate water storage. Also, a remote sensing technique called the Gravity Recovery and Climate Experiment (GRACE) has been developed to estimate water storage and evapotranspiration over a large scale by measuring the changes in gravity fields [27,28]. The mass of loess is, therefore, helpful for the verification of this method. As loess deposits on the LP are thick, they store large quantities of carbon and nutrients [14,29]. Current estimates of carbon and nutrients in loess have been mainly derived from the upper layers [30], so unknown amounts of carbon and nutrients have been missed by these estimates. Although the deep loess carbon and nutrients are not easily used by plants or released, they do play an important role in determining groundwater quality and biogeochemical cycling [30]. Hence, quantification of the mass of loess is needed to provide basic data to calculate the storages of water, carbon, and nutrients for promoting the sustainability of regional ecosystems and understanding regional eco-hydrological processes.

In this study, we used the loess thickness data, a pedotransfer function (PTF) for bulk density (BD), and the observed clay content data to estimate the loess mass across the LP from ArcGIS spatial analysis. The objectives of this study were to (1) demonstrate the procedure of loess mass estimate and (2) map the loess mass across the LP and evaluate its spatial distribution.

2. Materials and methods

2.1. Region of interest

The LP, with an area of 6.4×10^5 km^2, is located in the middle reaches of the Yellow River and is surrounded by four mountains: Qinling, Taihang, Yinshan, and Riyue (Fig. 1) [13,21]. The LP is not completely covered with loess due to heterogeneity in soil geneses and topography. The northwestern part of the plateau is mostly covered with aeolian sandy soil due to its proximity to the dust source and low precipitation. The westernmost part of the plateau is mainly covered with desert soil. The southernmost and easternmost parts are mountainous areas, and due to steep slopes and forest vegetation, the loess does not quickly accumulate there, so it is mainly stony soil. Combined, the areas above are called the typical loess region, which have an area of 3.6×10^5 km^2 (Fig. 1). The mountainous areas inside the typical loess region are also mainly stony soils, which have an area of 3.5×10^4 km^2, and these areas are not included in the loess mass estimate. Therefore, the region of interest (ROI) is the area covered by continuous and thick loess on the LP, with an area of 3.2×10^5 km^2.

2.2. Loess mass calculation

The mass of soil can be calculated by the BD and volume of the soil. In this study, we used a PTF to calculate the BD of loess [31]. The PTF is based on the soil core samples in five soil boreholes with a maximum depth of 204 m (Fig. 2a). This method was determined to be the best for predicting the BD of deep loess as it has a high determination coefficient ($R^2 = 0.356$) and a low root-mean-square error (0.079) [31]. The PTF has only two input parameters: clay content and loess depth (i.e., the distance to the surface). The clay content data was obtained from the upper 5 m of soil from 242 sites across the LP, and each site represented an area of 40 km × 40 km (Fig. 2a). The 0–5 m deep soil in each site was sampled at depths of 1, 2, 3, 4, and 5 m, and then the clay contents of the samples were determined in the laboratory using a laser diffraction particle size meter (Mastersizer 2000, Malvern Instruments, UK). The average clay content for these five depths represented the clay content of each site, and this ensured the representativeness of the clay content parameter input into the PTF. Then, we used the radial basic function interpolation method (RBFI) in ArcGIS (version 10.3, Esri Inc., USA) to generate a clay content distribution map with a resolution of 100 m × 100 m based on the average clay contents in the 242 sites (Fig. 2b). The standardized mean (SM) and standardized root-mean-square (SRMS) of the prediction error by the RBFI were 0.003 and 2.59, respectively, indicating that the interpolation method can meet the needs of this study.

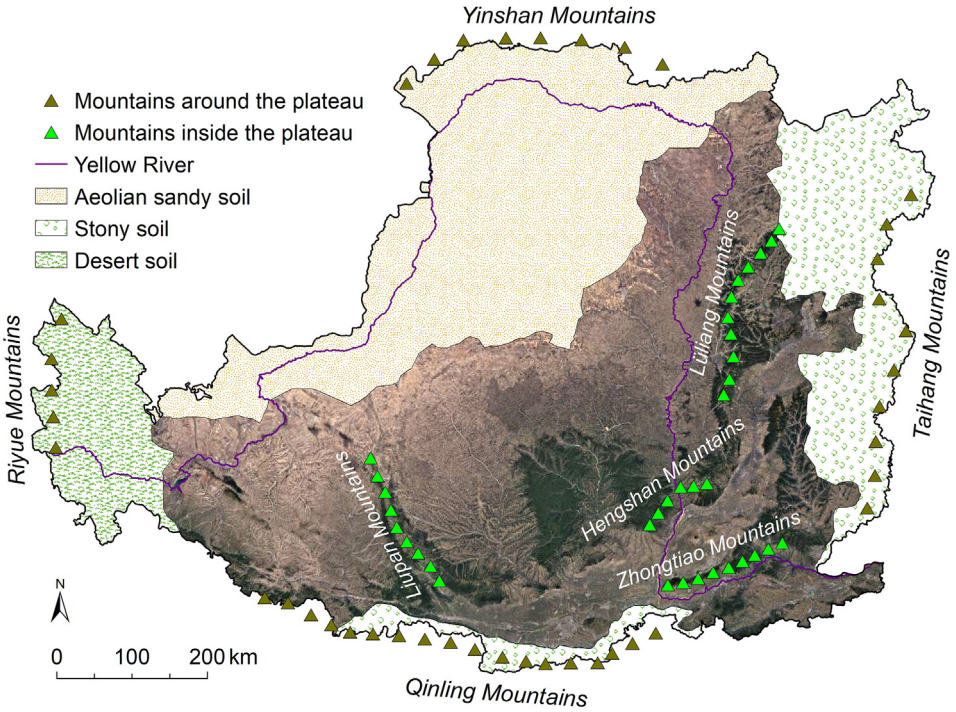

Fig. 1. The region of interest for loess mass determination.

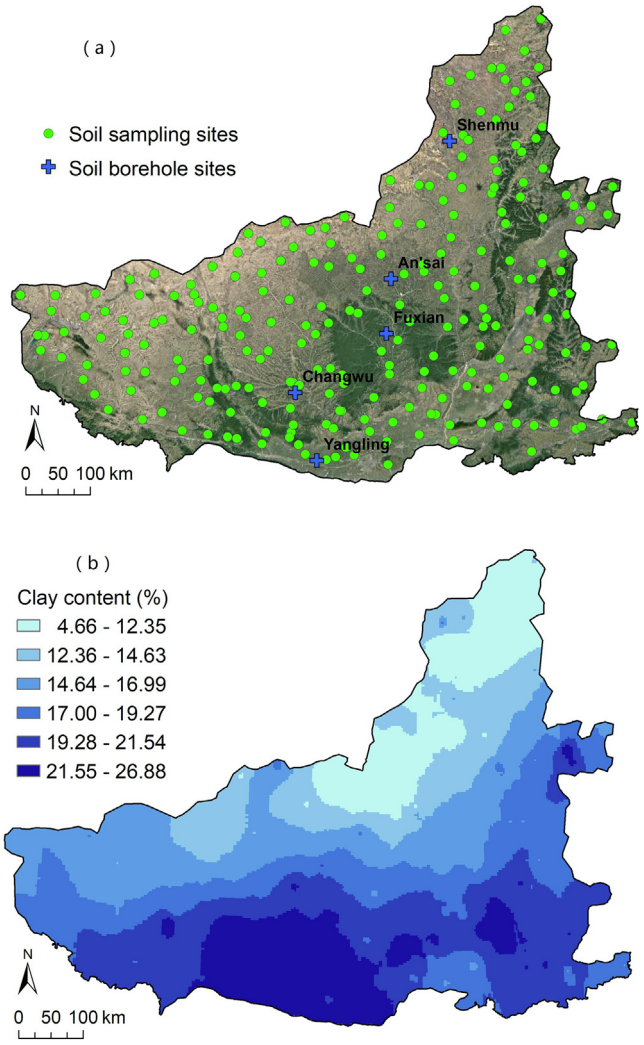

Fig. 2. Soil sampling and soil borehole sites (a) and the map of average clay content (b) across the Loess Plateau.

Next, we derived the loess depth based on a previous study of loess thickness [14]. That study used neighborhood analysis in ArcGIS and the observed loess thickness to obtain and verify the loess thickness across the LP. For details on the loess thickness estimate, the readers are referred to [14]. The resolution of the loess thickness map is 100 m × 100 m, which is consistent with the clay content map mentioned above. The loess thickness for a pixel on the loess thickness map has two meanings. The first indicates the maximum depth of the site corresponding to this pixel, and the second indicates the number of depths to be calculated (starting at 1 m with a depth interval of 1 m). For example, for a pixel with a loess thickness of 10 m, the maximum loess depth of the site is 10 m; the number of depths that should be calculated is 10, which are 1, 2, 3, ⋯, and 10 m. Using the method, we converted the loess thickness data into depth data, and combined the clay content data to calculate the BD of loess at different depths.

The BD of loess at a given depth at a site with a maximum depth of n m can be calculated by the following equation [31]:

$$BD_i = k \times \left(1.68 + 0.001 \times D_i - 2.249 \times C^{-1} - 0.086 \times D_i^{-1}\right), \quad (1)$$

where BD_i is the bulk density calculated at a depth of i (=2, 3, 4, ⋯, n) m at a site (g cm^{-3}), D_i is depth i in m, and C is the average clay content at a site (%). In this PTF, all variables are dimensionless, taking only their values. The parameter k is used to assign a unit to the calculated value (k = 1 g cm^{-3}).

The average BD of loess at a site can be calculated from:

$$\overline{BD} = k \times \left(1.68 - 2.249 \times C^{-1} + 0.001 \times \frac{\sum_1^n D_i}{n} - 0.086 \times \frac{\sum_1^n D_i^{-1}}{n}\right), \quad (2)$$

where $\overline{BD}$ is the mean bulk density of loess at a site (g cm^{-3}).

Eq. (2) can be simplified as

$$\overline{BD} = k \times \left(1.68 - 2.249 \times C^{-1} + 0.001 \times \frac{n+1}{2} - 0.086 \times \frac{(\ln(n+1)+a)}{n}\right), \quad (3)$$

where a is the Euler's constant (≈0.5772).

The loess mass over an area of 1 m^2 which can be calculated from:

$$W_j = (k_0 \times \overline{BD_j}) \cdot d_j \cdot A_0, \quad (4)$$

where W_j is the loess mass for the jth pixel on the map (t), $\overline{BD_j}$ is the average bulk density for the jth pixel on the map (g cm^{-3}), d_j is the maximum depth of the jth pixel on the map (m), k_0 is the coefficient used to translate g cm^{-3} into t m^{-3} (=1 t m^{-3} g^{-1} cm^3), and A_0 is the given area (=1 m^2).

The total loess mass can be written as

$$W_t = A \times \sum W_j, \quad (5)$$

where W_t is the total loess mass of ROI (t) and A is the area of ROI (m^2).

Using Eq. (3) and the average clay content map, combined with the map algebra method, we derived a map of the average BD across the LP. Finally, using Eq. (4), the average BD map, and the loess depth data, we derived a map of loess mass across the LP using the same method.

3. Results

3.1. Spatial distribution of bulk density across the Loess Plateau of China

The PTF for BD and easy-to-obtain clay content data were combined using ArcGIS spatial analysis to generate a loess distribution map of the average BD (Fig. 3). The results showed that the average BD of loess between the surface and bedrock is 1.58 g cm^{-3}, ranging from 1.18 to 1.87 g cm^{-3}. The south-central part of the LP had the largest BD (blue circle), river valley areas were relatively smaller (black dotted circles), and the northwest was the smallest (green circle). The histogram of BD versus area indicates that the BD of loess was a non-normal distribution, which can be fitted by the Gaussian model (Fig. 3a). The peak of the BD was offset to the right side of the horizontal axis. The dominant BD was between 1.53 and 1.62 g cm^{-3} (gray area in Fig. 3a). There was a hyperbolic relationship between BD and the loess depth (Fig. 3b), indicating that the BD was positively related to the loess depth. The BD of loess is greater than previously estimated, and the maximum BD was up to nearly 1.9 g cm^{-3}.

To verify the reliability of the calculated BD by the PTF, we used the five soil boreholes from the surface to the bedrock extracted from Yangling, Changwu, Fuxian, An'sai, and Shenmu (Fig. 2a). The maximum depth of the boreholes was 204 m. Then, intact soil cores were extracted from the boreholes to obtain the real BD of loess between the surface and bedrock (Fig. 4). The real BD of loess was found to increases with increased depth. The real BD of the topsoil was between 1.2 and 1.4 g cm^{-3}, and the maximum was 1.9 g cm^{-3}. The relationship between the real BD and the loess depth can also be fitted by the Gaussian model. The range of variation of the real BD is consistent with our calculated BD, indicating that the calculated BD by the PTF is reliable and accurate.

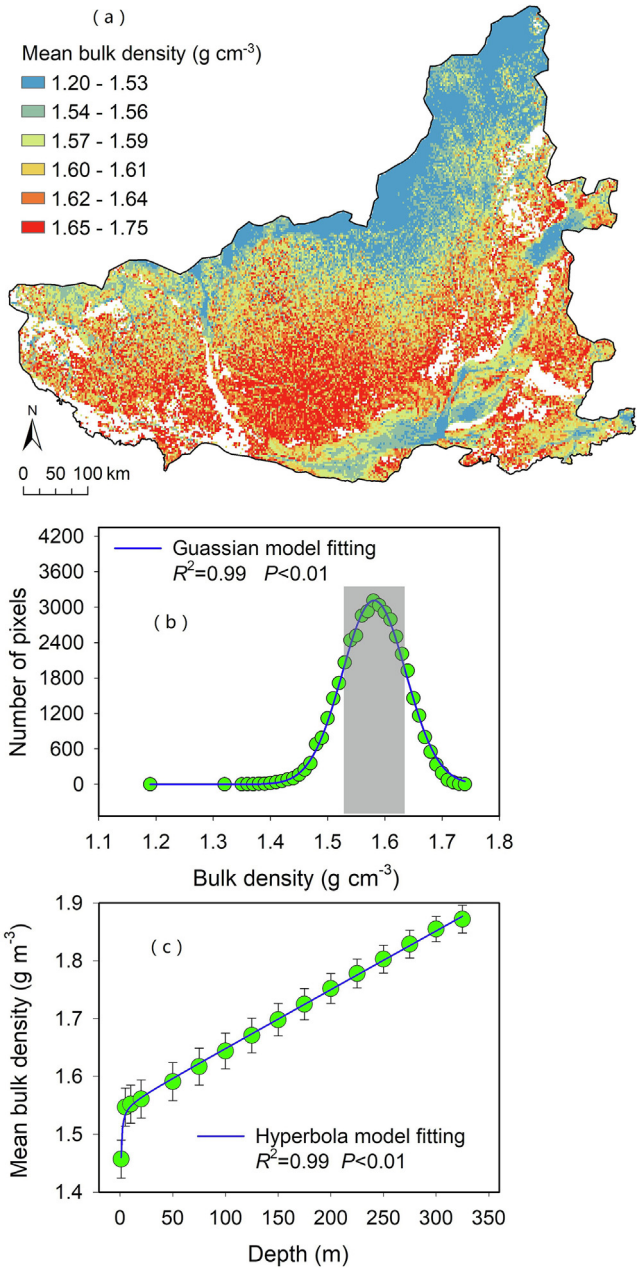

Fig. 3. Bulk density of loess and its statistical and variation characteristics. (a) Distribution map of mean bulk density across the Loess Plateau, (b) histogram of bulk density by the number of pixels, and (c) the relationship between mean bulk density and depth.

3.2. Spatial distributions of loess mass across the Loess Plateau of China

Based on the distribution map of loess mass across the LP (Fig. 5), we estimated the total mass of loess on the LP to be 5.45×10^{13} t. The average loess mass over an area of 1 m^2 was 169 t, which varied from 1.36 to 585 t. The loess mass in the south-central part of the LP was the greatest (white circle), and in the northwest borderline (black dotted line) and river valley areas (black circle), the loess mass was relatively small (Fig. 5). This uniform distribution of loess mass is shown in the histogram of loess mass versus area (Fig. 5a). The cumulative probability curve of loess mass per square meter with 0.25 and 0.75 probability lines is shown in Fig. 5b. The intersection points of the lines with the curve corresponded two values of 161 and 314 t m^{-2}, respectively.

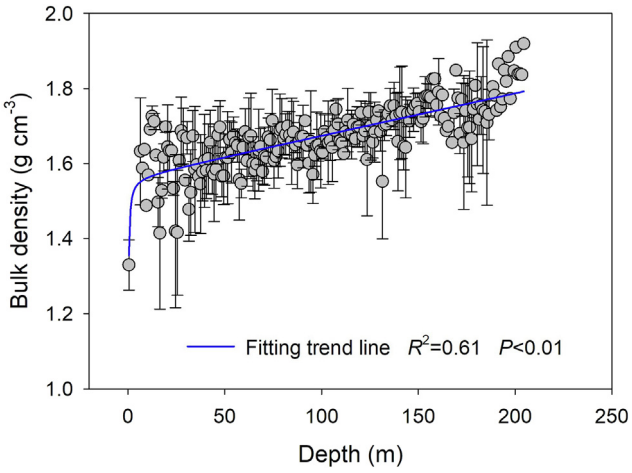

Fig. 4. Observed bulk density of the loess between the surface and bedrock from the five soil boreholes on the Loess Plateau.

These two values are divided by the average BD of loess in the LP (1.58 g cm^{-3}, or 1.58 t m^{-3}) which showed that the dominant loess thickness on the LP is between 101.9 m (=161 t m^{-2}/1.58 t m^{-3}) and 198.7 m (=314 t m^{-2}/1.58 t m^{-3}).

4. Discussion

The BD of loess enabled us to calculate the mass of loess. Due to the difficulty in sampling deep loess, we used a PTF to calculate the BD in the deep loess. We extracted intact soil cores between the surface and bedrock from five soil boreholes with a maximum depth of 204 m to determine the real BD of loess. Our observed and calculated BDs all indicated that the BD of loess is higher than previously estimated, averaging 1.58 g cm^{-3}. When the loess depth exceeded 300 m, the BD was greater than 1.85 g cm^{-3}, and the maximum BD was close to 1.9 g cm^{-3} (Figs. 3b and 4). The high BD in the deep loess is mainly due to the thick loess deposits in the LP, as the large weight load upper loess compressed the deeper layers. According to our calculations, the weight per square meter on the lowest loess is up to 585 t, and its pressure is 5.7×10^6 Pa, i.e., 50 standard atmospheric pressure. With such tremendous pressure, the lowest loess will be strongly compressed, resulting in the observed high BD. The BD of deep loess is high, and the corresponding soil porosity will therefore be small. Therefore, the water and solute transport in deep loess will be, in theory, slow. Therefore, when simulating the water and solute transport in the deep loess profile, we cannot use the BD of the upper loess to replace the BD of the deep loess, as this will lead to unreliable results.

The spatial distribution map of loess mass shows the regional differentiation of loess accumulation. We can roughly determine the average accumulation rate of loess (without considering the erosion of loess) since the Quaternary geological period (i.e., 2.6 Ma) based on our estimate of loess mass [32], and it is 2.1×10^7 t a^{-1}. The area where we estimated the mass of loess is generally the main source area of sediment being deposited into the Yellow River. Comparing this value with the annual average sediment of the Yellow River Basin into the sea (2.56×10^8 t a^{-1} for 1987–2015) [19], we estimate that the current erosion rate of the LP is higher than the average accumulation rate, indicating that the LP thickness will continue to decrease due to soil erosion. Therefore, we recommend that measures be taken to reduce soil erosion in addition to vegetation restoration and check dam construction, which have helped control soil erosion in the region over the past 20 years.

Our estimated loess mass helps to verify the results of GRACE. Schnitzer et al. [33] used two GRACE solutions, and estimated the

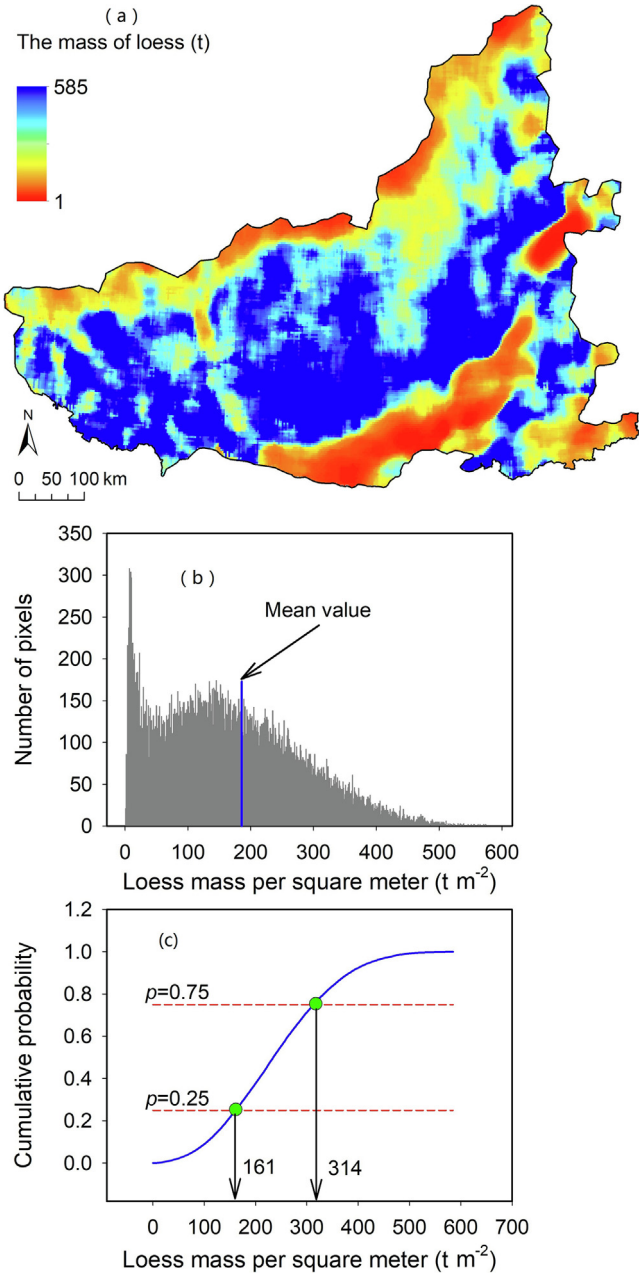

Fig. 5. Mass of loess and its statistical characteristics. (a) Distribution map of loess mass across the Loess Plateau, (b) histogram showing distribution of loess mass by area, and (c) a cumulative probability curve of loess mass per square meter where $p = 0.25$ and $p = 0.75$ represent the 0.25 and 0.75 probability lines, respectively.

annual average mass changes in the LP to be 11.7 Gt for 2003–2009 (ITG-Grace2010 solution) and 4.84 Gt for 2005–2011 (GFZ-RL05 solution). The average of these two numbers gives an estimate of the multi-year average mass change of the LP as 8.27 Gt, or 8.27×10^9 t. The area used in their estimate is 6.0×10^5 km^2, and the area of this study is 3.2×10^5 km^2. In this case, the annual mass change of this study area calculated by the GRACE should be 4.41×10^9 t (or 4.41 Gt = 8.27 Gt×(3.2×10^5 km^2/6×10^5 km^2)). Since the root depth of most plants in the LP is less than 5 m and the infiltration depth of precipitation is less than 3 m, we divide the loess profile into two layers: the surface layer (the upper 5 m loess) and the deep layer (the >5 m loess). The surface loess is affected by precipitation and vegetation, while the deep loess is not affected by these factors. Under these assumptions, it can be concluded that the mass change of the LP mainly comes from the

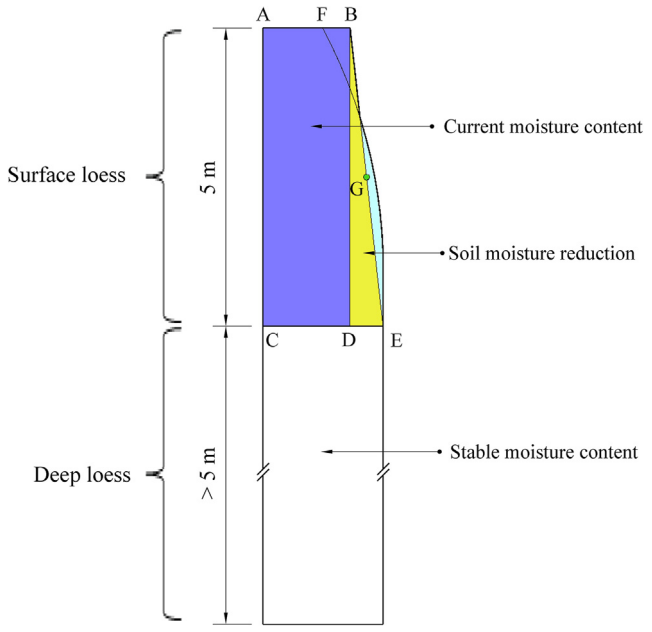

Fig. 6. Soil moisture profile of the loess and change of soil moisture.

change in water storage in the surface loess. Based on the average BDs for the surface and the deep loess (1.3 and 1.59 g cm^{-3}, respectively) and the average loess thickness (105.7 m) [14], the ratio of surface loess mass to the total loss mass is around 0.039 (=5 m × 1.3 g cm^{-3}/(5 m × 1.3 g cm^{-3} + 100.7 m × 1.59 g cm^{-3})), and consequently the mass of upper 5 m loess is 2.13×10^{12} t (=5.45×10^{13} t × 0.039). According to our unpublished data (2013), the average soil moisture contents (SMC) in the deep loess layer and the surface loess layer, named the stable SMC and the current SMC, respectively, were 0.201 cm^3 cm^{-3} (E point in Fig. 6) and 0.146 cm^3 cm^{-3} (B point in Fig. 6), respectively. We assumed (1) the SMC in the upper 5 m loess increases linearly from the current SMC to the stable SMC (a straight line B-E in Fig. 6), and (2) after a 15-year vegetation restoration (1999–2013), the water in the region of a triangle B-D-E was consumed (the actual moisture profile may not be a straight line B-E, but an arc F-E, see Fig. 6). With this assumption, we calculated the rate of soil moisture reduction to be about 0.00183 cm^3 cm^{-3} a^{-1} (=(SMC_G-SMC_B)/duration of years = (0.201 cm^3 cm^{-3} + 0.146 cm^3 cm^{-3})/2–0.146 cm^3 cm^{-3})/(2013–1999 + 1), where SMC_G is the SMC in G point, SMC_B is the SMC in B point in Fig. 6. G point is the middle point of straight-line B-E)). This indicated that the proportion of soil water reduction per year is 0.00183. When multiplied by the mass of the upper loess, the annual change of water storage in the LP is equivalent to 3.90×10^9 t, which is close to 4.41×10^9 t (the result of the GRACE). Our calculated change in water storage in the LP is less than the result of the GRACE, because the latter includes not only water storage, but also groundwater, runoff, and sediment.

The uncertainties of this study are associated with the PTF we selected, the observed clay content of the upper 5 m loess, the loess thickness data, and the spatial interpolation method we used. First, the PTF that was selected is suitable for estimating BD in areas with thick loess deposits because the PTF is based on soil core samples with a maximum depth of 204 m. Although it does not reach the maximum depth of the LP (about 350 m), it represents most of the LP. Also, in the PTF, the weight of depth is greater than that of clay content. Therefore, if the depth is accurate, the calculated BD should also be relatively accurate. Our observed BD values match well with the predicted values, and as the depth increases, the BD increases, and the deep BD was well predicted (Fig. 4). Second, for the PTF to provide an accurate estimate of BD, we mea-

sured the clay content of the upper 5 m loess at the 242 sites across the LP and used the average clay content to ensure more reliable input of clay content data, which is, to some extent, more representative. Third, the loess thickness data was obtained using ArcGIS neighborhood analysis and the DEM of the LP. The calculated thickness data was verified by the observed data of 162 sites across the LP [14]. The calculated average thickness is 105.7 m, slightly higher than was observed, which may result in a slight overestimation of the loess mass. Fourth, when performing spatial interpolation, we choose the RBFI method without considering the spatial dependence between the sample data, which is simple and direct, and the SM and SRMS satisfy the needs of this study. Finally, we used the estimated loess mass to verify the results of the GRACE, and they are close, indirectly indicating the relative accuracy of our estimate on the loess mass.

5. Conclusion

We calculate the BD of loess by using a PTF, the observed clay content data, and the loess thickness data, and then estimate the mass of loess and its distribution across the LP. The average BD of loess between the surface and bedrock is 1.58 g cm^{-3}, ranging from 1.18 to 1.87 g cm^{-3}. The south-central part of the LP has the largest BD, river valley areas are relatively small, and the northwest is the smallest. The total loess mass on the LP is 5.45×10^{13} t, the average mass of loess over an area of 1 m^2 is 169 t, with a range of 1.36–585 t. The loess mass in the south-central of the LP is the largest, and that in the northwest and river valley areas is relatively small. Our estimate of loess mass enables us to calculate water, carbon, and nutrients stored in the LP, which is the basis for understanding soil-water processes and ecohydrological systems in the LP.

Conflict of interest

The authors declare that they have no conflict of interest.

Acknowledgments

This work was supported by the National Natural Science Foundation of China (41571130081, 41371242, 41530854), the Youth Innovation Promotion Association of the Chinese Academy of Sciences (2017076), the Youth Innovation Research Team Project (LENOM2016Q0001), and the Open Research Fund of State Key Laboratory of Soil Erosion and Dryland Farming on the Loess Plateau (A314021402-1806). We thank the editor and the reviewers for their comments and suggestions to improve this paper.

Author contributions

Yuanjun Zhu designed this paper, analyzed the data, and made all maps. Xiaoxu Jia provided clay content data in 242 sites and suggested the frame of the paper. Jiangbo Qiao helped to run the pedotransfer function. Ming'an Shao provided constructive suggestions on the paper.

References

[1] Schlesinger WH, Jasechko S. Transpiration in the global water cycle. Agric Forest Meteorol 2014;189–190:115–23.
[2] Jobbágy EG, Jackson RB. The uplift of soil nutrients by plants: biogeochemical consequences across scales. Ecology 2004;85:2380–410.
[3] Cavagnaro TR. Soil moisture legacy effects: impacts on soil nutrients, plants and mycorrhizal responsiveness. Soil Biol Biochem 2016;95:173–7.
[4] Apollo M, Andreychouk V, Bhattarai SS. Short-term impacts of livestock grazing on vegetation and track formation in a high mountain environment: a case study from the Himalayan Miyar valley (India). Sustain 2018;10:951–7.
[5] Fu B, Wang S, Liu Y, et al. Hydrogeomorphic ecosystem responses to natural and anthropogenic changes in the Loess Plateau of China. Annu Rev Earth Planet Sci 2017;45:223–43.
[6] Wang S, Fu B, Piao S, et al. Reduced sediment transport in the Yellow River due to anthropogenic changes. Nat Geosci 2016;9:38–44.
[7] Kosmas C, Danalatos N, Cammeraat LH, et al. The effect of land use on runoff and soil erosion rates under Mediterranean conditions. Catena 1997;29:45–55.
[8] Chen J. Rapid urbanization in China: a real challenge to soil protection and food security. Catena 2007;69:1–15.
[9] Xu Y, Zhang Y, Lin E, et al. Analyses on the climate change responses over China under SRES B2 scenario using PRECIS. Chin Sci Bull 2006;51:2260–8.
[10] Liu C, Huang W, Feng S, et al. Spatiotemporal variations of aridity in China during 1961–2015: decomposition and attribution. Sci Bull 2018;63:1187–213.
[11] Montgomery DR. Soil erosion and agricultural sustainability. Proc Natl Acad Sci USA 2007;104:13268–75.
[12] Pimentel D, Harvey C, Resosudarmo P, et al. Environmental and economic costs of soil erosion and conservation benefits. Science 1995;267:1117–27.
[13] Liu T. Loess and the environment. Beijing: Science Press; 1985 (in Chinese).
[14] Zhu Y, Jia X, Shao M, et al. Loess thickness variations across the Loess Plateau of China. Surv Geophys 2018;39:715–813.
[15] Jia X, Shao M, Zhu Y, et al. Soil moisture decline due to afforestation across the Loess Plateau. China. J Hydrol 2017;546:113–210.
[16] Lü H, Liu D, Guo Z. Natural vegetation of geological and historical periods in Loess Plateau. Chin Sci Bull 2003;48:411–6.
[17] Pécsi M. Loess is not just the accumulation of dust. Quat Int 1990;7:1–21.
[18] Frechen M, Oches EA, Kohfeld KE. Loess in Europe-mass accumulation rates during the Loess Glacial Period. Quat Sci Rev 2003;22:1835–43.
[19] Yellow River Sediment Bulletin in 2016. Yellow River Conservancy Commission of the Ministry of Water Resources; 2016.
[20] Pimentel D. Soil erosion: a food and environmental threat. Environ Dev Sustain 2006;8:119–219.
[21] Tang K. Soil and water conservation in China. Beijing: Science Press; 2004 (in Chinese).
[22] Li D, Du S, Wu L, et al. An overview of soil loss tolerance. Catena 2009;78:93–7.
[23] Lal R. Soil carbon sequestration impacts on global climate change and food security. Science 2004;304:1623–5.
[24] Johnson CM, Vieira ICG, Zarin DJ, et al. Carbon and nutrient storage in primary and secondary forest in eastern Amazônia. Forest Ecol Manage 2001;147:245–8.
[25] Yao Y, Piao S, Wang T. Future biomass carbon sequestration capacity of Chinese forests. Sci Bull 2018;63:1108–10.
[26] Li Z, Chen X, Liu W, et al. Determination of groundwater recharge mechanism in the deep loessial unsaturated zone by environmental tracers. Sci Total Environ 2017;586:827–9.
[27] Rodell M, Famiglietti JS. An analysis of terrestrial water storage variations in Illinois with implications for the Gravity Recovery and Climate Experiment (GRACE). Water Resour Res 2001;37:1327–413.
[28] Swenson S, Wahr J, Milly PCD. Estimated accuracies of regional water storage variations inferred from the Gravity Recovery and Climate Experiment (GRACE). Water Resour Res 2003;39:1223–8.
[29] Jia X, Zhu Y, Huang L, et al. Mineral N stock and nitrate accumulation in the 50 to 200 m profile on the Loess Plateau. Sci Total Environ 2018;633:999–1008.
[30] Wei X, Shao M, Fu X, et al. Distribution of soil organic C, N and P in three adjacent land use patterns in the northern Loess Plateau, China. Biogeochemistry 2009;96:149–214.
[31] Qiao J, Zhu Y, Jia X, et al. Development of pedotransfer functions for predicting the bulk density in the critical zone on the Loess Plateau, China. J Soil Sediment 2018;18:1–7.
[32] Ding Z, Yang S, Sun J, et al. Re-organization of atmospheric circulation at about 2.6 Ma over northern, China. Quat Sci 1999;47:277–85 (in Chinese).
[33] Schnitzer S, Seitz F, Eicker A, et al. Estimation of soil loss by water erosion in the Chinese Loess Plateau using Universal Soil Loss Equation and GRACE. Geophys J Int 2013;193:1283–8.

Yuanjun Zhu is an associate professor of Northwest A&F University. His research focuses on the water process in the deep vadose zone of the Loess Plateau to improve our understanding of regionally hydrological and ecological systems.